32nd URSI GASS, Montreal, 19–26 August 2017

Full Wave Analysis of Chaotic Reverberation Chambers

L. Bastianelli[(1)(2)], G. Gradoni[(2)(3)], F. Moglie[(1)], V. Mariani Primiani[(1)]
(1) DII - Università Politecnica delle Marche, Ancona, Italy
(2) School of Mathematical Sciences, University of Nottingham, Nottingham, UK
(3) George Green Institute for Electromagnetics Research, University of Nottingham, Nottingham, UK

Abstract

In this paper, we study possible ways to improve the Reverberation Chamber (RC) behavior. There could be benefits in deforming the RC rectangular geometry of the baseline cavity by inserting spherical diffractors into the RC or by titling the walls of the RC. We demonstrate that increased field disorder and randomization can be achieved with both the asymmetric structures in presence of the same mechanical stirrer. It is found that the improvement is prominent at low frequencies, with respect to the lowest usable frequency (LUF), which is consistent with results obtained by other investigators on similar RC structures. Numerical Finite-Difference Time-Domain (FDTD) simulations are performed to demonstrate the field chaoticity improvement in terms of both uncorrelated excitation frequencies and stirrer configurations.

1 Introduction

The Reverberation Chamber (RC) is an overmoded rectangular cavity which is widely used in Electromagnetic Compatibility (EMC) tests and emulation of the Rician channel in wireless communications [1, 2]. In order to validate the RC operation a few performance indicators have been defined and are usually measured to assess the level of mixing/randomization of the chamber field [3]. The lowest usable frequency (LUF) is an empirical parameter that gives the RC operator an estimate of a lower bound for overmodedness [4]. Improving the operation of an RC at frequencies below the LUF, or even reducing the LUF itself, is an important task for the statistical electromagnetics community [5, 6]. The foundations for a physically-motivated definition of LUF are still to be achieved, and constitute an exciting challenge. Obviously, increasing the dimensions of the baseline cavity is an easy way to reduce the LUF. However, such a practice hampers the realization of compact and cost-effective RCs. Furthermore, one needs to shed light on the statistical physics of few cavity eigenmodes. The LUF is defined as the $3-6\times f_0$, where f_0 is the frequency of the fundamental mode of the cavity that depends on the dimensions of the RC. In order to create chaotic fields within the cavity, different kind of stirring methods can be adopted. The most used one is the mechanical stirrer, i.e. an irregular metallic structure. Beyond this limit, the RC is well behaved [7] and the field is statistically uniform, isotropic and depolarized within a spatial region defined as Working Volume (WV). Another possible way to improve the RC's behavior, or to reduce the LUF, is to deform the shape of the cavity. This work has been pioneered in [12, 13, 14] with the innovative proposal of adding spherical diffractors on the walls of an RC. Field disorder has been evaluated by means of Random Matrix Theory approach (RMT) [8, 9, 12, 13, 14].

2 FDTD Simulations

Simulations are done by using our reliable parallel code that implements the FDTD technique, and runs on supercomputer [10, 11]. The FDTD is easily parallelizable and is well suited for HPC facilities. Each stirrer position, corresponding to a RC realization, runs on a computer node by means MPI directives. Then in each node the code is further parallelized by means OpenMP.

2.1 Spherical diffractors

The dimensions of the RC are $6\times4\times2.5$ m^3, we hereafter preserve the volume of the original RC even in presence of spherical diffractors. The frequency of the fundamental mode is found to be $f_0\simeq45$ MHz. We simulated two discone antennas in order to study the scattering parameters, S_{21}, over a broad frequency range. Figure 1 shows the simulated RC, the vertical z-folded stirrer and a sphere placed between the wall and the floor. The investigated band is

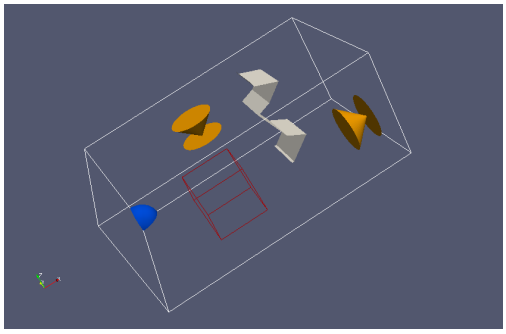

Figure 1. Simulated RC, equipped by two discone antennas and stirrer. Moreover a spherical diffractor, $1/8$ of a whole sphere was inserted. The red box represents the WV.

$0.2 \div 1.0$ GHz. In our simulations, the cell size is 3 cm so the whole RC was sampled by $201 \times 134 \times 84$ cubic cells. We simulated 128 stirrer positions (2.81°) and 512 frequencies in each sub-band of 31.25 kHz. Moreover, we simulated walls, antennas stirrer and spherical diffractors as PEC whereas losses are added in the air which a value of $\sigma = 10^{-5}$ S/m [11]. The chosen cell size corresponds to $\lambda/10$ at 1 GHz and the time step is 50 ps. With inserting spheres, they affect behavior inside the RC, altering the waves propagation in order to improve the field mixing. The improvement depends both on the combination

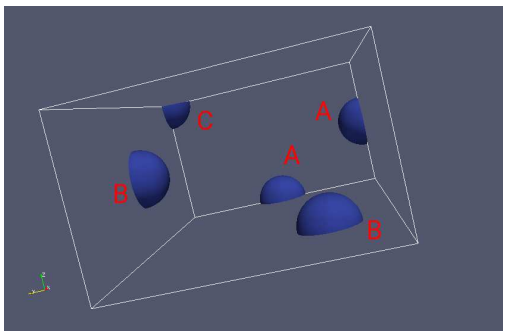

Figure 2. Picture of possible placement of spherical diffractors into the RC.

and positions of sphere, also increasing them by increasing the radius. The insertion of spherical diffractor also affect total volume, V, of the RC then the Q-factor, defined as

$$Q = \frac{16\pi^2 V \langle |S_{21}|^2 \rangle}{\lambda^3 \eta_{Tx} \eta_{Rx} \left(1 - |\langle S_{11} \rangle|^2\right) \left(1 - |\langle S_{21} \rangle|^2\right)} \qquad (1)$$

with c the speed of light in the vacuum, V the volume of the RC and f the frequency, S_{21} is the complex scattering transmission coefficient, whereas S_{11} and S_{22} are the complex scattering reflection coefficients. The antenna efficency coefficients η_{Tx} and η_{Rx} for the Tx and Rx antennas respectively, are ≈ 1 because simulated as PEC and well matched. The performances are evaluated by means of the uncorrelated frequencies by using the multivariate approach [15]. We construct a correlation matrix whose entries represent correlation coefficients between RC (total) fields obtained at pairs of frequencies or stirrer positions ("events"). Then the Pearson's correlation coefficients are computed in the following way

$$\rho_{jk} = \frac{\mathrm{Cov}\left(\underline{e}^{(j)}, \underline{e}^{(k)}\right)}{\sqrt{\mathrm{Var}\left(\underline{e}^{(j)}\right) \mathrm{Var}\left(\underline{e}^{(k)}\right)}}, \qquad (2)$$

where e_j and e_k are two random field vectors of the matrix of the events at different frequency positions, j and k respectively, and $Cov(\cdot,\cdot)$ stands for the covariance and $Var(\cdot)$ for the field variance. Finally the total number of uncorrelated frequencies are given by the number of values in the correlation matrix greater than the threshold value of the IEC standard

$$N_u = \frac{N_f^2}{\#\left[\underline{R} > r\right]}. \qquad (3)$$

Figure 3 reports the number of uncorrelated frequencies when a spherical diffractor is placed on a bottom corner of the RC. There is a increase of the uncorrelated frequencies beyond 400 MHz. It is worth noting that increasing the number of diffractors within the RC causes a more remarkable improvement of the behavior of the chamber. The more the diffractors the more the occupied volume into the RC. In our code, the number of inserted spherical diffractors can be varied according to the available volume for further EMC test including devices. Diffractor shape and positioning can be varied, e.g. corner sphere ("C"), floor/ceiling or wall sphere ("B"), between two walls of the RC ("A") or a mixed combination of previous, see Figure 2. Different diffraction positions makes it different in terms of results and occupied volume. In order to validate the chamber, the

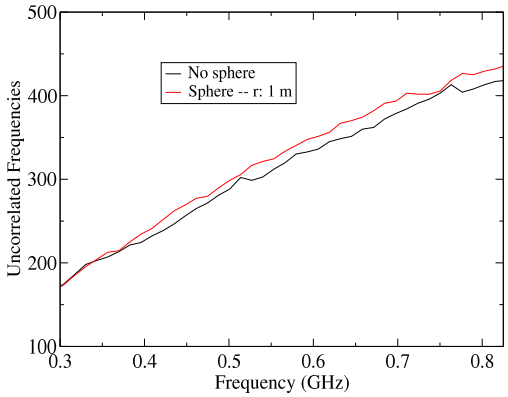

Figure 3. Comparison of the number of uncorrelated frequencies between a RC without diffractors and with one sphere placed between two walls.

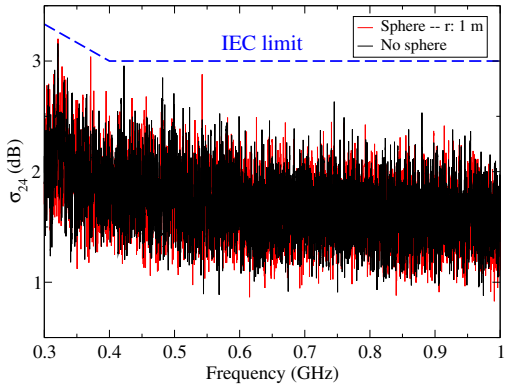

Figure 4. Simulated standard deviation of the original RC, and when one sphere on the corner was inserted in it. The IEC-standard limit is reported.

field uniformity was checked [3]. The standard deviation, reported in eq. (4), provides the values within the tolerance accepted by the normative [3], [16]. The standard deviation in (dB) is expressed by

$$\sigma_{24}(dB) = 20log\left(\frac{\sigma_{24} + \langle E_{x,y,z} \rangle}{\langle E_{x,y,z} \rangle}\right) \qquad (4)$$

where the σ_{24} is the standard deviation evaluated on 24 probe positions, 8 for each Cartesian component, and $\langle E_{x,y,z} \rangle$ is the arithmetic mean of the normalized E_{MAX} from all 24 probe positions. Figure 4 shows the evaluated standard deviation of the original RC and the same RC when a sphere is added as depicted in Figure 1. Values of the standard deviations meet the standard limit [3] throughout the investigated band.

2.2 Tilted walls

The dimensions of the RC are $4 \times 5 \times 3$ m^3, the same volume are preserved also when walls are tilted. The frequency of the fundamental mode is found to be $f_0 \simeq 48$ MHz. We simulated two discone antennas in order to study the scattering parameters, S_{21}. Figure 5 shows the simulated RC, vertical z-folded stirrer is used and walls are tilted. The

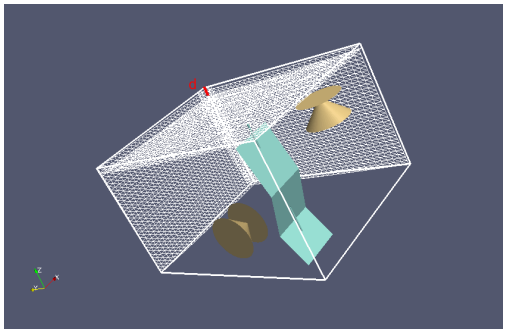

Figure 5. Simulated RC where three walls are tilted through the RC. There are two discone antennas and a z-folded stirrer. The penetration through the RC is set by the parameter d.

investigated band is $0.2 \div 2.0$ GHz. In our simulations, the cell size is 1.5 cm so the whole RC was sampled by $401 \times 268 \times 168$ cubic cells. Walls are tilted by means spheres centered very far from the RC. The penetration of the walls through the RC can be varied. We simulated walls, stirrer as Perfect Electric Conductors (PEC) whereas losses are added in the air which a value of $\sigma = 10^{-5}$ S/m. The chosen cell size corresponds to $\lambda/10$ at 2 GHz and the time step is 28 ps. We simulated 512 stirrer positions (0.70°). The number of uncorrelated stirrer position are evaluated by using the Auto Correlation Function (ACF). The correlation coefficient is calculated as

$$r = \frac{\frac{1}{N-1}\sum_i^N (x_i - u_x)(y_i - u_y)}{\sigma_x^2 \sigma_y^2} \qquad (5)$$

and then compared with the IEC threshold [3]. The x_i and y_i represent the received power where y_i is shifted by one w.r.t. x_i for each stirrer position, whereas u_x and u_y are the mean of received power, and finally σ^2 is the variance and N is the number of samples. Figure 6 reports the number of uncorrelated stirrer position when three walls are tilted by a penetration $d = 35$ cm. We can note that the improvement slowly begin at about 300 MHz and it is more marked over 1 GHz. Figure 7 reports the field uniformity of eq. (4),

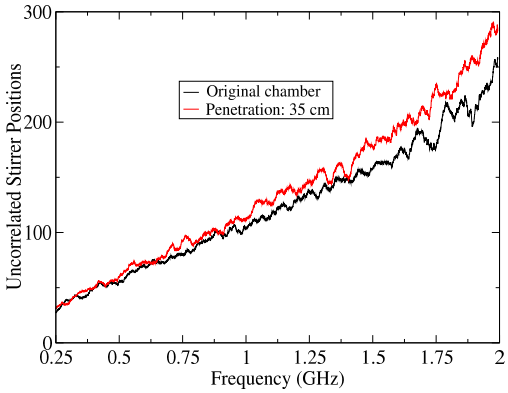

Figure 6. Number of uncorrelated stirrer positions when walls are tilted by 35 cm. A sliding average window over 400 frequency points has been used.

evaluated for the original RC and for the same one with tilted walls, as in Figure 5. Tilting the walls of the chamber involved some frequencies in exceed the IEC limit, especially at low frequency, below 300 MHz. These peaks are due to the walls closer to the WV with respect to the original RC. However, we considered more frequency points than the required by the standard. The improvement of the new geometries can be appreciated in terms of an increase of the number of uncorrelated stirrer positions in frequency, as shown in Figure 6. Now we are focusing on the evaluation of eigenvalues, i.e. resonant frequencies of the RC take advantage of the wave chaos theory. Considering ideal conductive walls distribution of these eigenmodes are already treated [17]. Another key parameter under investigation, is

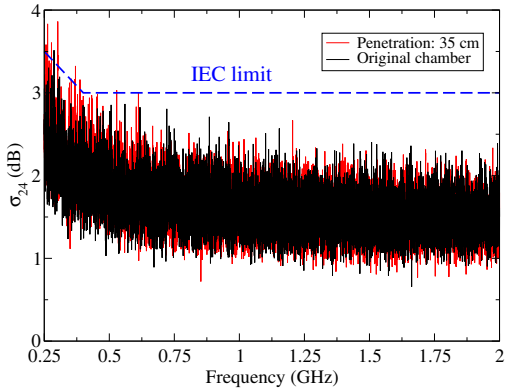

Figure 7. Simulated standard deviation of the original RC and walls tilted by 35 cm. The IEC standard limit is reported.

the inverse participation ratio (IPR) that is able to evaluate the degree of localization of the field [18]. The IPR evaluated in a regular RC is greater with respect to a chaotic one, where regular modes are predominant.

3 Conclusions

Wall deformations or tilting improve the overal behaviour of standard reverberation chambers. In particular deform-

ing the rectangular geometry increases the chamber field chaoticity. The improvement is evaluated by typical parameters used for RC analysis, such as uncorrelated stirrer positions by means of the ACF and uncorrelated frequencies by means of the multivariate approach. The improvement depends on both number and positions of the sphere, or in the case of tilted walls on the penetration depth through the RC. This study confirms independent findings from other investigators and are preliminary to understanding the role of regular modes surviving the stirring mechanism.

4 Acknowledgments

This work was supported by a STSM Grant from COST Action IC1407 (ACCREDIT). We acknowledge PRACE for awarding us access to resource FERMI based in Italy at CINECA. L. Bastianelli acknowledges the School of Mathematical Sciences, University of Nottingham, for hospitality. We thank Olivier Legrand (Nice) for the fruitful discussions.

References

[1] C. L. Holloway, D. A. Hill, J. M. Ladbury, G. Koepke, "Requirements for an Effective Reverberation Chamber: Unloaded or Loaded", *IEEE Trans. Electromagn. Compat.*, **48**, February 2006, pp. 187–194, doi:10.1109/TEMC.2006.870709.

[2] M. T. Ma, "Understanding reverberating chambers as an alternative facility for EMC testing" *Journal of Electromagnetic Waves and Applications*, **2**, 1988, pp. 339–351.

[3] "Electromagnetic compatibility (EMC) – Part 4-21: Testing and measurement techniques – Reverberation chamber test methods", *International Standards – IEC 61000-4-21, Geneva, Switzerland*, **2.0**, April 2011.

[4] F. Monsef, A. Cozza, "A Possible Minimum Relevance Requirement for a Statistical Approach in a Reverberation Chamber", *IEEE Trans. Electromagn. Compati*, **57**, December 2015, pp. 1728–1731, doi:10.1109/TEMC.2015.2464318.

[5] D. A. Hill, "Electromagnetic theory of reverberation chambers", *National Institute of Standards and Technology, Tech. Rep. NIST TN*, December 1998.

[6] L. R. Arnaut, "Operation of electromagnetic reverberation chambers with wave diffractors at relatively low frequencies", *IEEE Trans. Electromagn. Compat.*, **43**, November 2001, pp. 637-653, doi:10.1109/15.974645.

[7] P. Corona, G. Ferrara, M. Migliaccio, "Reverberating chambers as sources of stochastic electromagnetic fields", *IEEE Trans. Electromagn. Compat.*, **38**, August 1996, pp.348–356.

[8] U. Dörr, H. J. Stöckmann, M. Barth, U. Kuhl,"Scarred and Chaotic Field Distributions in a Three-Dimensional Sinai-Microwave Resonator– Phys. Rev. Lett.", *American Physical Society*, **80**, February 1998, pp. 1030–1033, doi:10.1103/PhysRevLett.80.1030.

[9] H.J.Stöckmann, "Quantum Chaos: An Introduction", *Cambridge University Press*, 2006.

[10] F. Moglie, "Convergence of the Reverberation chambers to the Equilibrium Analyzed with the Finite-Difference Time-Domain Algorithm", *IEEE Trans. Electromagn. Compat.*, **46**, 2004, pp. 469–476.

[11] F. Moglie, L. Bastianelli, V. Mariani Primiani, "Reliable Finite-Difference Time-Domain Simulations of Reverberation Chambers by Using Equivalent Volumetric Losses", *IEEE Trans. Electromagn. Compat.*, **58**, June 2016, pp. 653–660, doi:10.1109/TEMC.2016.2548520.

[12] J.-B. Gros, O. Legrand, F. Mortessagne, E. Richalot, K. Selemani, "Universal behaviour of a wave chaos based electromagnetic reverberation chamber", *Wave Motion* **51**, pp. 664–672, June 2014.

[13] K. Selemani, J.-B. Gros, E. Richalot, O. Legrand, O. Picon, F. Mortessagne, "Comparison of reverberation chamber shapes inspired from chaotic cavities", *IEEE Trans. Electromagn. Compat.*, **57**, pp. 3–11, February 2015.

[14] J.-B. Gros, U. Kuhl, O. Legrand, F. Mortessagne, O. Picon, E. Richalot, "Statistics of the electromagnetic response of a chaotic reverberation chamber", *Adv. Electromagn.*, **4**, 2015.

[15] G. Gradoni, V. Mariani Primiani, F. Moglie, "Reverberation chamber as a multivariate process: FDTD evaluation of correlation matrix and independent positions", *Progress In Electromagnetics Research*, **133**, 2013, pp. 217–234, doi:10.2528/PIER12091807.

[16] J.-B. Gros, U. Kuhl, O. Legrand, F. Mortessagne, P. Besnier, E. Richalot, "Tolerance requirements revisited for the calibration of chaotic reverberation chambers", *8ème colloque et expositions internationale sur la compatibilité électromagnétique (CEM 2016)*, pp. 359–362, July 2016.

[17] R. Balian, C. Bloch, "Distribution of eigenfrequencies for the wave equation in a finite domaina", *Electromagnetic field Riemannian spaces – Ann. Phys.*, **64**, pp. 271–307, 1971.

[18] K. Selemani, E. Richalot, O. Legrand, O. Picon, F. Mortessagne, "Energy localization effects within a reverberation chamber and their reduction in chaotic geometries", *IEEE Trans. Electromagn. Compat.*, **59**, pp. 325–333, April 2017.